UNSW Canberra

FINAL YEAR PROJECT

Automated Measurement of Ambient Electromagnetic Noise

Author:
SBLT Jordan Brown

Supervisor:
Dr. Greg Milford

A System for the Automated Measurement of Ambient Electromagnetic Noise

Jordan D Brown[1]
University of New South Wales at the Australian Defence Force Academy

There are three fundamental methods of communicating underwater; optics, acoustics and radio frequency electromagnetic waves. This project has focused on electromagnetic waves as they can penetrate the air/ water interface. As electromagnetic waves penetrate the air/ water interface, the noise under water is the same as that in the air, albeit attenuated. The goal of this project was to develop an efficient system for the continual measurement and analysis of (region specific) ambient EM noise. The analysis of this information will help develop an understanding of long-term diurnal and seasonal trends in order to optimise communication systems.

Contents

[1] SBLT, School of Engineering & Information Technology, ZEIT 4500/4501

Nomenclature

HF	High Frequency
LF	Low Frequency
RF	Radio Frequency
VLF	Very Low Frequency
ELF	Extremely Low Frequency
MF	Medium Frequency
UNSW	University of New South Wales
IEEE	Institute of Electrical and Electronic Engineers
EM	Electromagnetic
ITU	International Telecommunications Union
ksps	kilo samples per second
COTS	Commercial off the shelf
PCB	Printed Circuit Board
PSD	Power Spectral Density
UNSW	University of New South Wales
ADFA	Australian Defence Force Academy

Table 1-Table of Nomenclature

I Introduction

Radio frequency Electromagnetic (EM) waves are able to penetrate the air/water boundary without the need for wires. This trait is desirable if a system has receivers and transmitters on either side of this boundary; such as an aircraft communicating with a submarine. However, as frequency increases EM waves suffer greater attenuation reducing the transmission distance. This is overcome by transmitting at lower frequencies, which have less attenuation but also lower data rates. This relationship is described by the propagation coefficient; γ.The propagation coefficient is influenced by the conductivity, permeability and permittivity of the medium. In a lossless medium, like air, γ is purely imaginary ($\gamma = j\beta$); thus, there is no attenuation. However, in a lossy medium, such as sea water, γ is complex resulting in attenuation. Equation 1 reveals this relationship between an increase in frequency and attenuation.

$$\gamma = j\omega\sqrt{\epsilon\mu - j\frac{\sigma\mu}{\omega}} = \alpha + j\beta \quad (1)$$

It is hoped modern wireless multiple access techniques can increase these data rates. The goal of this project is to design a system which can measure and record the ambient electromagnetic noise both above and below water. It is intended that the analysis of these measurements will identify seasonal and diurnal trends, to provide the insight required to optimise the design for underwater communications systems.

A. Project Definition

This project is divided into two main sections. The first is a direct continuation of Alan Clarke's project from 2014. This, existing system was used to accumulate long term sets of data (in air); with the intention of exploring trends and feature extraction concentrating on the ELF to LF bands [1]. The second goal was to design an improved system, focusing on increased bandwidth and portability, in order to conduct measurements in salt water. As a result of this increased bandwidth this section focused on the VLF to MF bands [1]. The long term measurements in air are important to predict the signal strength (EM noise) in water.

II Background

This project has focused on the ELF to MF bands (0-2 MHz). These frequencies are traditionally used for navigation signals and communication with underwater systems (penetrating the air/water boundary). However, "radio noise sets a limit to the performance of radio systems."[2] Fundamentally, we must know the boundary conditions to optimise the system. The ITU defines noise as;

> *"a time varying electromagnetic phenomenon having components in the radio frequency range, apparently not covering information and which may be superimposed on, or combined with, a wanted signal."*[2]

A. Sources of ambient EM noise

This noise is divided into *natural* and *man-made* noise. Natural (environmental) noise at low frequencies (up to 100 KHz) emanates, predominantly, from lightning strikes [3]. At higher frequencies (VLF) galactic sources, particles and waves interacting with the magnetosphere, comprise a significant portion of EM ambient noise. In contrast, man-made noise is generated by technology such as power lines (50-60 Hz), electronic devices for indoor use or even car ignitions [4].

Additionally, the ITU-R lists the most prevalent forms of noise for radio systems (0.1 Hz to 100 GHz), these include;

- Radiation from lightning discharges (atmospheric noise due to lightning);
- Unintended radiation from electrical machinery, electrical and electronic equipments, power;
- transmission lines, or from internal combustion engine ignition (man-made noise);
- Emissions from atmospheric gases and hydrometeors;
- The ground or other obstructions within the antenna beam;
- Radiation from celestial radio sources

B. Noise and Frequency

The ITU recommendations reveal that external noise (F_a) given by equations 2 and 3 (Annex A) decreases with frequency. This relationship is shown at figure 1. In addition, while marginal, this noise has diurnal, seasonal and geographical variations. The solid curve (fig 1) represents the minimum hourly expected values of F_a while the dashed curve reveals the expected maximum values. This figure reveals there is very little diurnal variation at low frequencies (0-10 KHz), while at higher frequencies there is a higher degree of diurnal variation. This figure, and all ITU figures, provide an average of the world, and thus are not region specific. Finally, seasonal variation exists with the summer months having higher ambient noise due to increased atmospheric activity [3]. A comparison of summer and winter ambient noise is presented at Annex B.

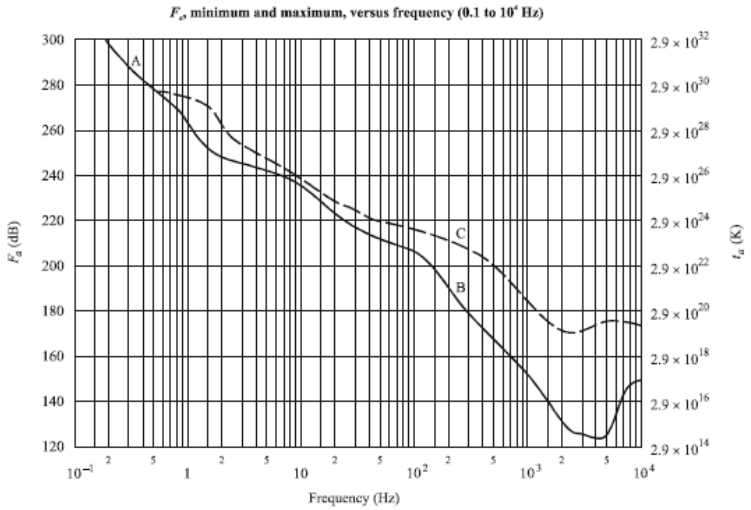

Figure 1- Noise (F_a) vs frequency

C. Best Practice

In 1985, the IEEE released standards for conducting an EM site survey (10 KHz to 10 GHz). This project has been conducted in accordance with the IEEE standards where possible. Deviations from this standard will be noted. A site is normally surveyed for one of two reasons; to characterise the performance of an existing or planned electronic system or to examine the potential contribution to short- and long-term biological effects [5]. This project is being conducted for the first of these reasons.

D. Site Survey

The IEEE divides site surveys into two general classifications; interior and exterior [5]. This project lies within the exterior measurement classification. The IEEE recommends the measurements scheduling should accommodate;

1. Normal operating hours of electrical and electronic equipment and broadcast transmitters
2. After-working-hours period when usage of equipment is minimal
3. Post-sunset interval when some broadcast transmitters operate at reduced power or cease transmission
4. Midnight-to-sunrise hours when some broadcast transmitters are inactive and when electrical usage and vehicular traffic are low.

In addition, equipment should be calibrated across the frequency range of interest for any receiver, detector or recorder. Furthermore, it recommends that a survey should be conducted over a period of at least two weeks with measurements taken each hour. This is done to establish a cyclical daily pattern.

III System Design

A. Existing System

The existing system, which was developed by Alan Clarke (2013), has been taking continuous measurements of ambient EM noise. It was designed as a modular system to reduce risk and allow for incremental improvement of the system. A block design of the system is presented at figure 2. The pre amplifier (orange box) was not integrated into the system due to a parasitic oscillation at 460 KHz. As the voltage induced at the antenna is very small (nano volts), the attenuation due to the transmission line presented a significant problem. Without the gain provided by the pre amplifier the noise of the Edirol above 48 KHz is greater than the strength of the received signal.

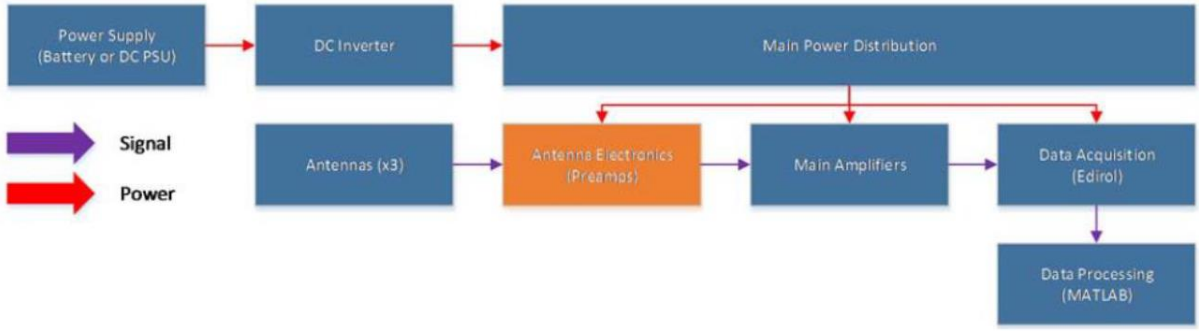

Figure 2-Block diagram existing system

B. New System

A block diagram of the improved system is presented at figure 3. The green box represents the equivalent circuit for the antenna.

Data Acquisition

The data acquisition is completed by the Terasic daughter board. The daughter board is an off the shelf (OTS) solution on loan from Dr Craig Benson. An AD 9248 ADC is integrated into the board. This is capable of sampling at 4 MS/S providing a bandwidth of 2 MHz. The daughter board is programmed to take a 1 second measurement every 20 s. This is contrast to the IEEE recommendations of a 1 minute measurement each hour. As the daughter board is an OTS solution, the alteration of the board's software was beyond the scope of this project.

Amplifier

A high impedance 5500Ω (measured) amplifier with a gain of 60 dB was utilised. The (high) impedance of the amplifier is important to reduce the effect described by the voltage divider rule (equation 4).

$$V_{source} = V_{in} \frac{R_{in}}{R_{in}+Z_s} \qquad (4)$$

Essentially, if the impedance of the antenna is sufficiently higher than the impedance of the amplifier the voltage measured at the ADC will be attenuated.

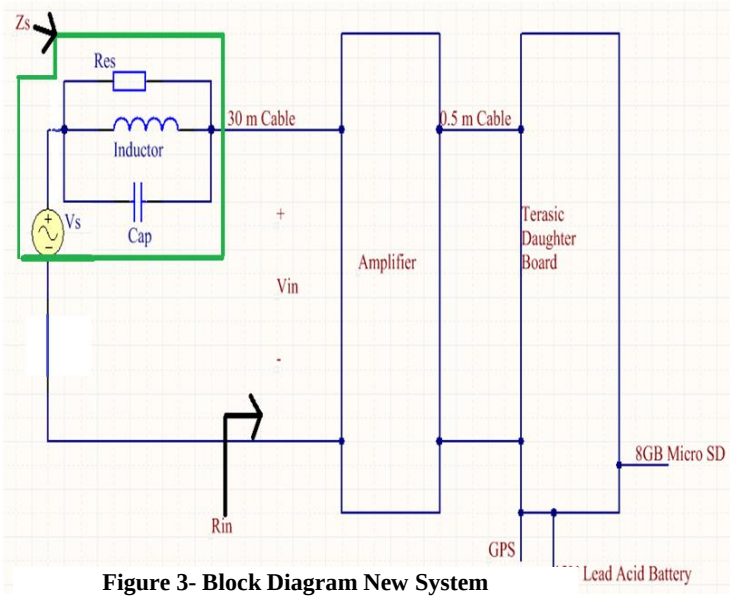

Figure 3- Block Diagram New System

Data Storage

The output of the ADC is stored on an 8 GB micro SD card as an unsigned 16 bit integer. This is capable of storing approximately 5 hours of data. Recorded data was transferred from the Micro SD card to a PC for long term storage.

Data Processing

The stored data is imported into MATLAB for processing. The raw data (nano volts) was processed using MATLAB's *pwelch* function to create a windowed PSD with 10241 bins.

C. Antenna Design (New System)

The antenna was designed as a loop antenna in accordance with the IEEE recommendations for measurements of frequencies below 30 MHz [5].

In order to design an efficient system, it is helpful to model the antenna as an equivalent circuit. In particular we want to model the source impedance (Z_s). The design process implemented in this project represents a parametric approach. The antennas impedance was measured on an E5071 C Network Analyser. The measured data was then compared to two heuristic equivalent circuits with stipulated component values. The measured data revealed resonant behaviour which indicated the model required a capacitive component. These models were series and parallel equivalent circuits. The model which best represented the measured data was a parallel RLC circuit (Figure 3). This circuit has the added advantage that we can model the real part of the impedance as the resistor value and the imaginary part of the impedance as the combination of the capacitor and inductor values. However, measured data is comprised by a combination of the desired signal and noise. In an attempt to remove the influence of the noise, the data was averaged across its surrounding measurements. This presents a trade-off as we are altering the measured data and potentially adding our own bias.

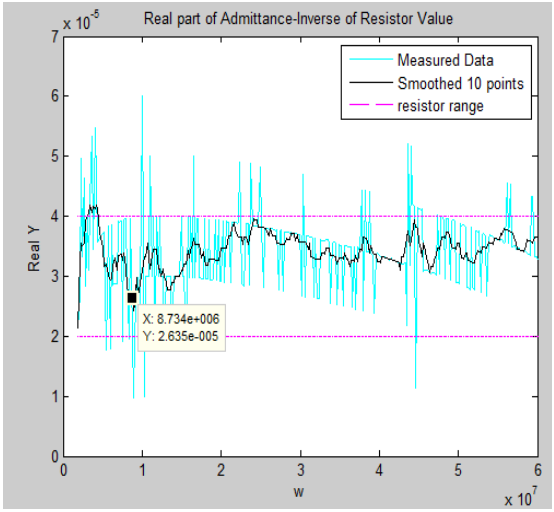

Figure 4-Resistor Value

Resistor

The resistor value can be modelled as the inverse of the real part of the admittance. Figure 4 displays a plot of the real part of the admittance vs the angular velocity (ω). In this plot the measured data is represented by the cyan line, while the averaged data is represented by the black line. The magenta lines represent the range of resistor values. This range represents an uncertainty due to the noise in the system. As R=1/Y, the resistor value for this circuit is 38KΩ.

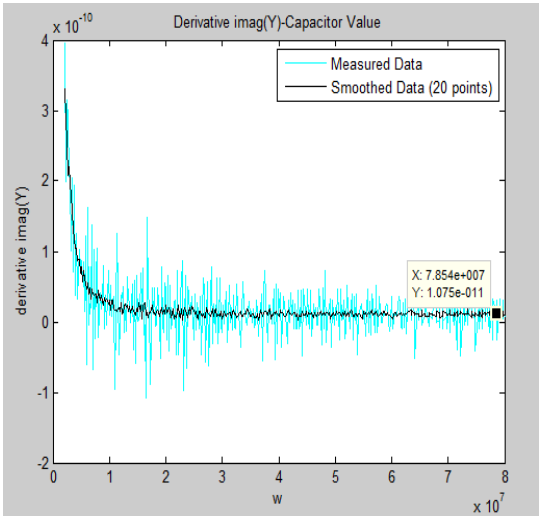

Figure 5-Capacitor Value

Capacitor

The capacitor value is determined from the derivative of the imaginary part of the admittance. As this value is obtained from the derivative of the imaginary part of admittance it is even more important to account for the noise. Figure 5 reveals the impact of the noise on the capacitor value (10pF).

Inductor Value

Once the capacitor value has been determined we can exploit the design of the parallel RLC circuit to determine the inductor value. Utilising equation 5, where F_r is the resonant requency;

$$F_r = \frac{1}{2\pi\sqrt{LC}} \quad (5)$$

The derived inductor value is 66 mH. We have now accounted for each of the component values.

D. Comparison of system performance

The existing system, while functional does provide some limitations.

Physical Limitations

Technically, the existing system is portable (it does not require mains power). However, while modular, the system has a significant number of components and is cumbersome to move. This is highlighted by the antenna design. The antenna system has a height of 1.5m, a width of 1 m and weighs 10 Kg. In contrast the new small loop ferrite antennas have a length of 15 cm, a diameter of 8mm and weigh 120g.

Performance Limitations

The ITU-R indicates there is very little seasonal variation below 10 KHz, this can be confirmed at figure 1. The bandwidth of the existing system (48 KHz), which is limited by the sampling rate and noise of the UA-101 Edirol, is relatively small. In contrast the new system has a bandwidth of 2 MHz; providing the necessary bandwidth to examine this phenomenon. A table comparing the performance of the two systems is presented at table 2.

	New	Existing
System	Tersasic Daughter Board (AD9248)	Edirol UA-101
Samplig rate	4Ms/S	192 Ks/S
Bandwidth	2MHz	48kHz
Storage	8GB Micro SD Card	1 TB external HDD
Measurement	1s /20s	1m/hour
Accuracy	14bit	24 bit (16bit used)
Max	3V	16dBu ≈4.8V (RMS)
Resolution	183uV	73.2uV
power requirements	12 V lead acid battery	12V DC/12V lead acid battery
signal levels	nano Volts	nano Volts

Table 2-Comparison (Existing v New System)

Antenna Specification (New System)

Employing the design process described at part C of this section, a parametric approach was applied to develop the most efficient antenna. Table 3 provides the key elements from the equivalent circuits. The two lines highlighted in yellow represent the same small loop air coil antenna. The antennas impedance was measured on the network analyser with and without a ferrite core. If we examine the two inductor values we can see the ferrite increases the inductor value by a factor of 60. This is important as, in accordance with Faraday's Law (equation 6), the voltage induced at the antenna (source voltage) is proportional to the change in flux.

$$V_{source} = L\frac{d\varphi}{dt} \quad (6)$$

Furthermore, the addition/removal of the ferrite does not alter the capacitor value. This should be expected as the capacitor value is representative of the proximity and configuration of the turns of the antenna. The two rows highlighted in pink represent two antennas with the same number of turns. However, they have different lengths (40 and 150 mm). To achieve the same number of turns; the turns on the shorter antenna were overlapped. The equivalent circuits reveal the longer antenna has more than twice the inductance, lower capacitance and a higher resonant frequency when compared to the shorter antenna. To summarise the table; as the number of turns increases the inductance increases (increasing antenna sensitivity) and the capacitance increases resulting in a lower resonant frequency.

No of Turns	Length(mm)	Ferrite	Turns Overlapped	Diameter (mm)	Resonant Frequency (KHz)	Equivalent Components		
						Resistor (Ω)	Inductor (H)	Capacitor (F)
50	150	Y	N	8	4429	5.00E+04	1.77E-04	7.70E-12
100	40	Y	Y	8	2069	5.00E+04	3.10E-04	1.90E-11
100	150	Y	N	8	2600	3.80E+04	6.66E-04	1.00E-11
185	**160**	**Y**	**Y**	**unknown**	**486**	**1.00E+04**	**7.40E-04**	**1.50E-10**
200	150	N	N	8	8753	4.00E+04	3.24E-05	1.00E-11
200	150	Y	N	8	1173	7.00E+04	1.90E-03	1.00E-11

Table 3-Antenna Comparison

The coils impedance is very large at resonance. Equation 4 reveals that this will result in an attenuated signal; effectively reducing the systems bandwidth. For these reasons the final antenna designed was a 100 turn with ferrite core (length 150mm). This design represented the best compromise between size, sensitivity and accuracy.

E. Calibration

The calibration for the antenna was conducted using air measurements taken from the roof of building 16 at the University of New South Wales at ADFA. In order for the measurements to be meaningful it is essential that the system is calibrated. Figure 6 displays this calibration process.

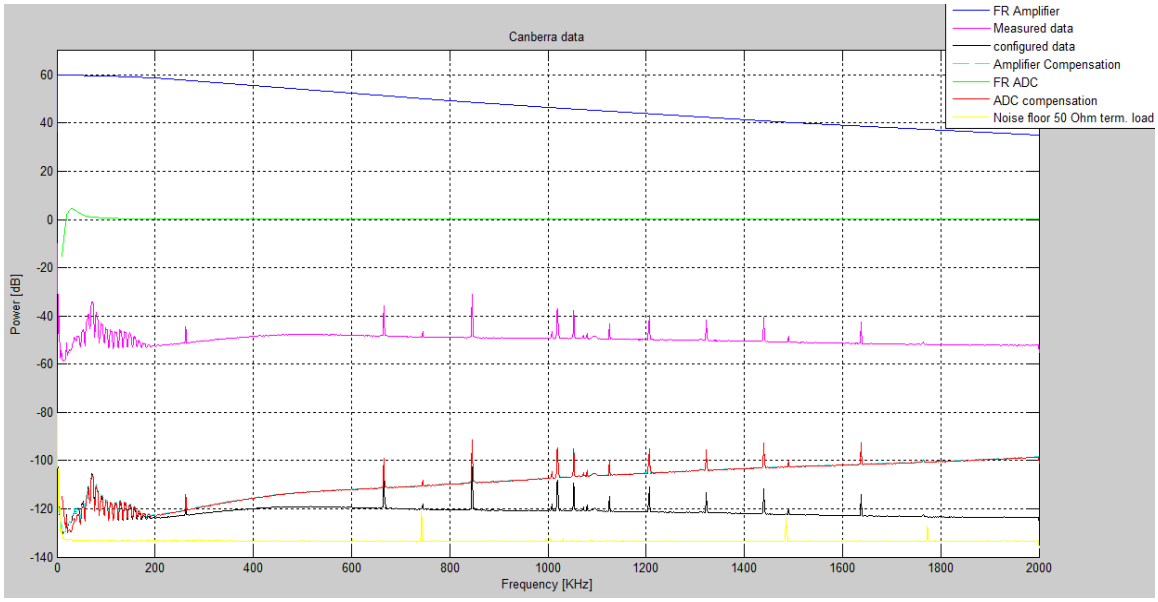

Figure 6-New system Calibration Process

Amplifier Frequency Response (blue line)

The blue line represents the frequency response of the amplifier. This was measured utilising a function generator (10 mV input voltage) and an oscilloscope. The dB value was calculated as a ratio of input to output voltage ($20LOG10(V_{out}/V_{in})$).

ADC Frequency Response (green line)

The ADC's frequency response was measured utilising a sinusoidal input voltage of 1 $V_{p\ to\ p}$. This was recorded on the ADC and processed in the time domain with MATLAB; the peak to peak voltage was then measured and recorded. This process was repeated over a range of frequencies. The flat portion of the frequency response ($8000_{p\ to\ p}$ (ADC reading)) was set as the base line and considered to represent 1 $V_{p\ to\ p}$ (0 dB). This baseline enabled a comparison between each of the measured values and 0 dB.

Un-calibrated PSD (magenta line)
The magenta line represents the PSD calculated directly from the data stored on the micro SD card.

Calibrated PSD (black line)
The ratio determined when calculating the ADC's frequency response was then applied to the raw numbers obtained from the SD card. The PSD was recalculated with the calibrated data.

Correction for Amplifier Roll off (cyan line)
The pass band of the Amplifier is 60 dB. A linear interpolation of the amplifier's frequency response was conducted to ensure it had the same number of points as the PSD. The difference between the amplifier's frequency response and 60 dB was calculated. This value was added to the Calibrated PSD.

Correction for ADC roll-off (red line)
In a similar manner to the amplifier correction the difference between the ADC frequency response and 0 dB was calculated. This value was applied to create the final calibrated response. Once calibrated the induced voltages measured at the antenna ranged from 1nV to 100nVs. The increase in V_s is in accordance with Farraday's Law. If we integrate equation 6, we derive equation 7.

$$|V_{source}(w)| = L\varphi w \qquad (7)$$

In which it is apparent that the source voltage induced at the antenna is frequency dependent (in air).

System Noise (yellow line)
The system noise was calculated by calculating the PSD when the amplifier was not connected. A 50Ω terminating load was placed across the ADC input.

IV Air and Seawater Measurements

The results section is split into two parts; the existing system and the new system.

A. Existing System

The existing system has been taking continual measurements from March 2014 to October 2014. This is completed with the intention of compiling long term data to explore trends and conduct feature extraction.

Diurnal Variation

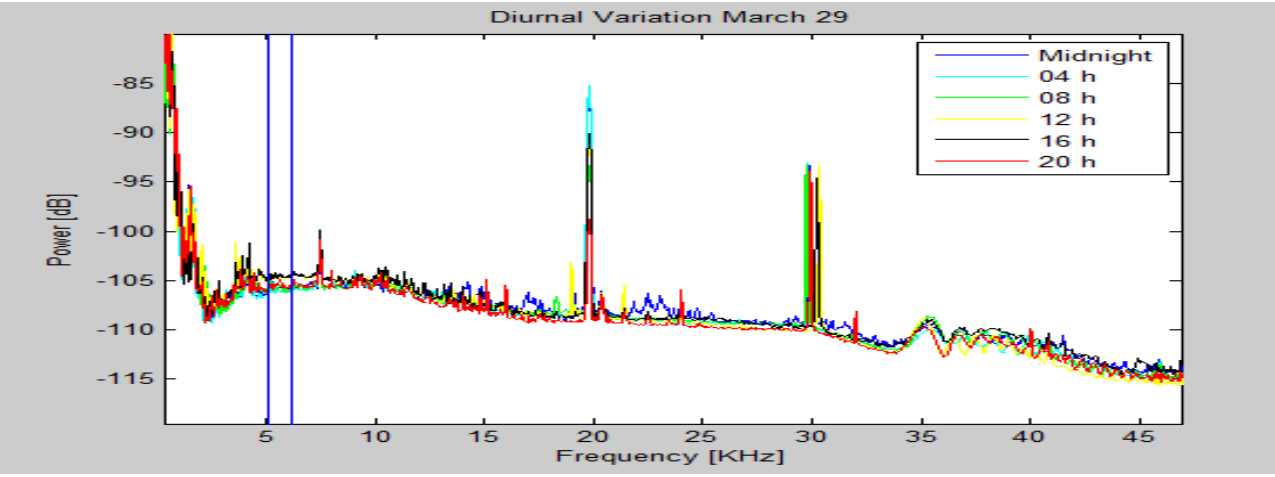

Figure 7-Broadband view of diurnal variation

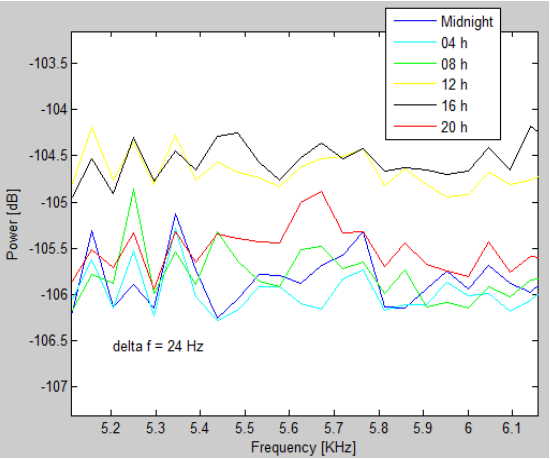

Figure 8-Diurnal Variation

Figure 7 presents a broadband view of diurnal variation. This is shown to provide an appreciation of the wider spectrum. Figure 8, provides a view of the frequency range between the solid blue lines (5-6 KHz). Figure 8 displays the diurnal variation over the course of one day (March 29, 2014). It confirms that the background noise is lowest between midnight and 8 am and higher during the daylight hours. This should be expected, as there are fewer weather events and less man-made noise at night [3]. In contrast, during the day there is both more man made noise and atmospheric noise due to an increased number of weather events [3].

Seasonal Variation

Figure 9 displays the broadband seasonal variation. The figure on the right (figure 10) displays the same information focusing on two frequencies; 18 and 23.44 KHz. In this plot the numbers on the bottom represent the month (ie March = 3). Each of the plots in figure 9, and their corresponding points on Figure 10 are representative of measured data obtained at 1800 h on the 29th day of each month. These plots reveal an increase in background noise in the winter months.

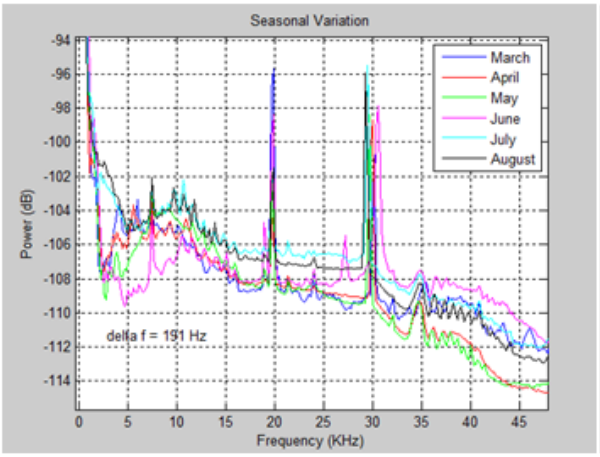

Figure 9-Broadband Seasonal Variation

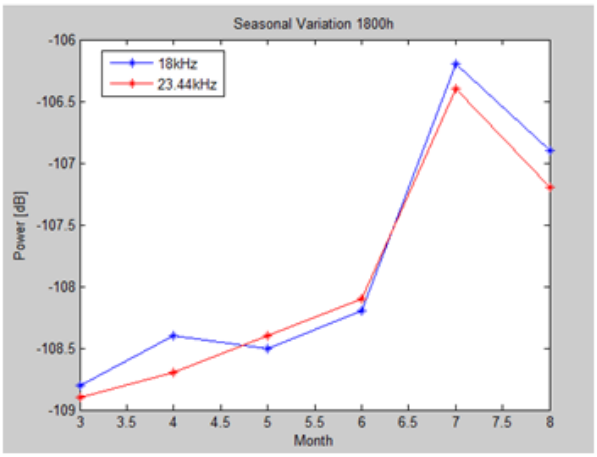

Figure 10-Seasonal Variation 18KHz/23.44KHz

This is unexpected; the ITU-R predicts higher levels of background noise in the summer months. However, it should be noted that the ITU-R data represents averages for the whole word. The period of increased noise (our winter) corresponds to the northern hemisphere summer, it is feasible that with greater land mass and thus greater weather related activity, the effect of the northern hemisphere summer accounts for this result.

Man-made variation

The Take Charge and Move Out (TACAMO) is a US military communication system. Figures 11 and 12 reveal the changing frequencies used by the system at different times of the year.

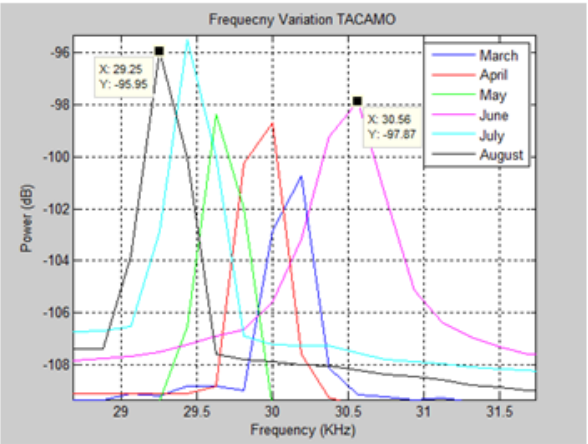

Figure 11- Variation TACAMO

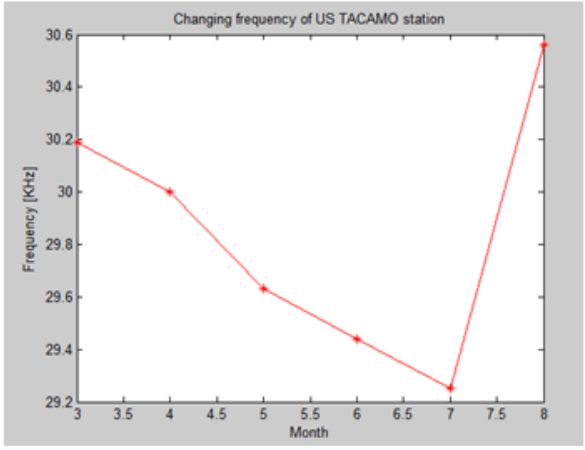

Figure 12-Frequency Variation TACAMO

B. New System

On Wednesday the first of October the system was transported to Huskisson, NSW to obtain salt water measurements. The location was a small jetty running parallel to the shore. This jetty projected 1m from the shore and the water had a depth of approximately 2m. To reduce risk (waterproofing) an antenna designed by Dr Robin Dunbar was used for these measurements. The same procedure for designing the equivalent circuit was carried out on this antenna (185 turn antenna table 3). The plots displayed at figure 13 display these initial measurements. Unfortunately due to boat traffic these results were obtained in two groups. The measurement obtained just under the water's surface and at a depth of 0.5 m were taken at 1130 am; the other measurements were taken at 1230 pm. These preliminary measurements have generated a lot of questions. These results represent a very small sample set and express the need for further measurements.

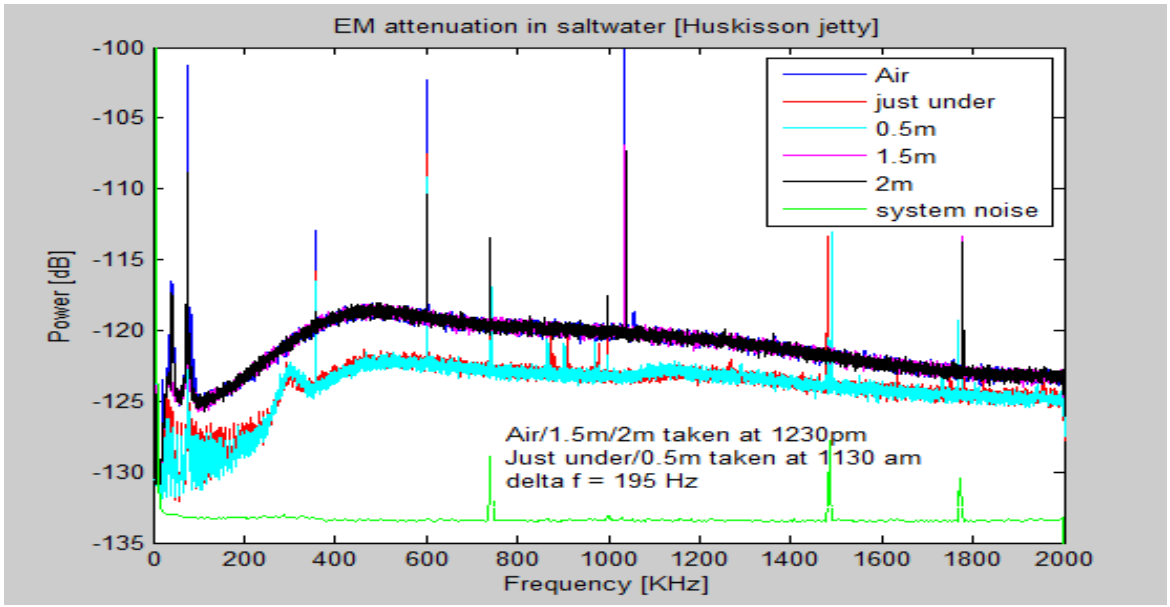

Figure 13-Salt water measurements (Huskisson)

Figure 14 represents a subset of figure 13, in which it focuses on ABC radio national (603 KHz). As such the disturbance between the measurements remains. However, within each of the groups of measurements there is attenuation with depth; with the exception of the measurement obtained at a depth of 2m. This measurement was taken on the bay floor; it is reasonable to expect an increase due to signals transmitted through the ground. This plot reveals an attenuation of 5dB/m at 500 KHz.

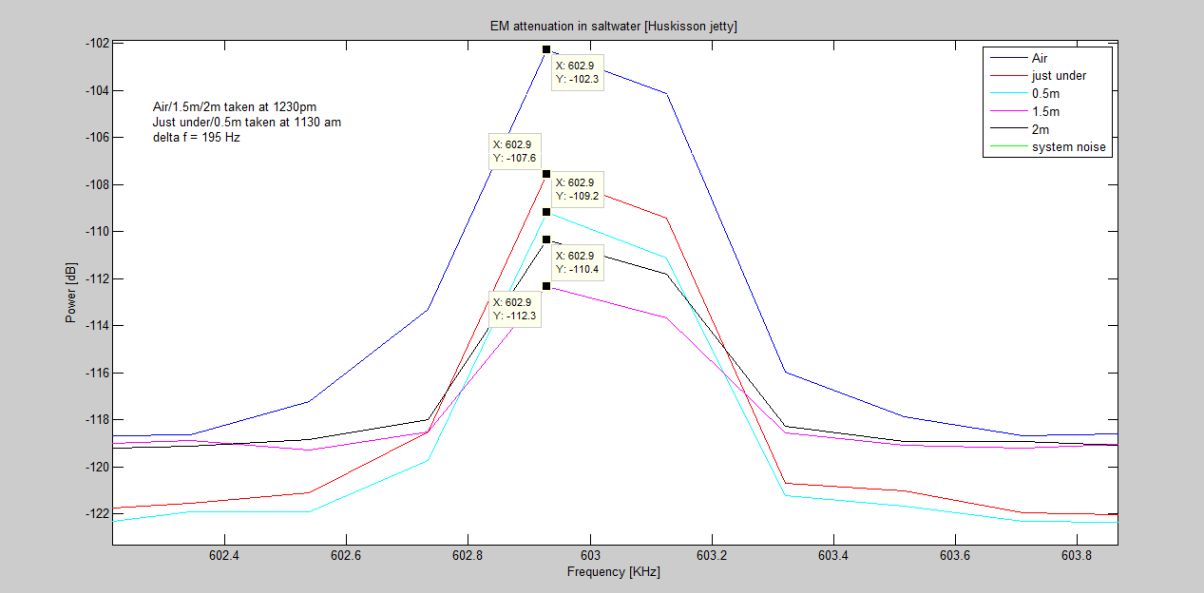

Figure 14- Attenuation Radio National 603KHz

V Conclusion

This project has been completed in two phases. The first was the maintenance of the existing system to develop a comprehensive data set. This data set spanned the months of March to October 2014. The analysis of this data has confirmed seasonal, diurnal and geographic variation. In addition it has been possible to analyse specific features; including the diurnal variation of the Harold E Holt antenna and the changing frequencies of the TACAMO system.

The second phase was to develop an improved system to conduct measurements under salt water. This project has successfully increased the bandwidth of the system from 48 KHz to 2 MHz. Furthermore, the system is significantly less cumbersome (more portable) than the existing system. The new system has been successfully employed in the saltwater environment; confirming the attenuation of ambient EM noise with depth.

This project has confirmed the dynamic nature of ambient EM noise. It varies diurnally, seasonally, geographically and in some cases (TACAMO) to serve a purpose. However, this noise attenuates with depth (in salt water). If we can find the optimum depth to minimise the atmospheric noise while at the same time minimising the attenuation of a desired signal, we can maximise the bandwidth and thus increase the data rate of underwater communications.

VI Recommendations

The new system has greatly increased the measureable bandwidth. However, the Terasic Daughter board, being an OTS solution is not designed for the continual measurement of ambient EM noise. The board should be reprogrammed to take measurements in accordance with the IEEE recommendations (1min/hour). Furthermore, the storage device (8GB micro SD card) is insufficient to conduct long term automated measurements. It is recommended that a USB interface be integrated into the board so the data can be stored on an external hard drive or PC. This would provide the means to accumulate a long term data set of the noise both above and below water. The higher bandwidth achieved with the new system is necessary to examine the increased influence of diurnal and seasonal variation at higher frequencies.

It is recommended that a more comprehensive analysis is conducted in the underwater environment. The initial measurements have provided some encouraging results; however, they highlight the need to accumulate a more comprehensive set of data.

Acknowledgements

The completion of this project would not have been possible without the support of a number of people. I would firstly like to thank my supervisor Dr Greg Milford for his support and guidance during this long and challenging project.

I would also like to thank my wife for her support over an incredibly challenging and exciting period of our lives.

Additionally, I would like to thank Dr Craig Benson and Dr Robin Dunbar. Dr Benson was willing to loan the Terasic Daughter board and surrounding system, while Dr Dunbar loaned a waterproofed antenna making the saltwater measurements possible.

Finally,I would like to thank Daryl Budarick for his support and technical assistance. He provided an invaluable resource and was always willing to help even on short notice.

References

[1] ITU Radio Regualtions. Volume 1, Article 2; Edition of 2008. Available online at http://life.itu.int/radioclub/rr/art02.htm

[2] ITU, 2008, *ITU Recommendation P. 372-9*

[3] Maxwell, E. & Stone, D., 1963. Natural Noise Fields From 1 cps to 100 kc. *IEEE Transactions on Antennas and Propagation,* p. 343.

[4] C. Bianchi and A. Meloni, "Natural and Man-made Terrestrial Electromagnetic Noise: An Outlook," *Annals of Geophysics*, vol. 50, 2007

[5] IEEE, "IEEE Recommended Practice for an Electromagnetic Site Survey (10 kHz to 10 GHz)," tech. rep., IEEE 1992.